RSC Advances

COMMUNICATION

Cite this: *RSC Adv.*, 2015, **5**, 26806

Received 24th February 2015
Accepted 5th March 2015

DOI: 10.1039/c5ra03391h

www.rsc.org/advances

Organic amorphous hole-transporting materials based on Tröger's Base: alternatives to NPB†

Ishita Neogi,[a] Samik Jhulki,[a] Madhu Rawat,[b] R. S. Anand,[b] Tahsin J. Chow[c] and Jarugu Narasimha Moorthy*[a]

Tröger's Base (TB) scaffold has been exploited to create two novel amorphous hole-transporting materials (HTMs), *i.e.*, **TB1** and **TB2**, with high T_gs (152–156 °C) as alternatives to the popular NPB ($T_g \sim 95$ °C). The hole-transporting properties of both **TB1–2** are shown to be comparable to or better than that of NPB by contrasting the results of device fabrications with two different emissive materials that are TB-based and non-TB-based. This in conjunction with the ease of synthesis of **TB1–2** should render them appealing choices as HTMs.

The advantages that the organic light-emitting diodes (OLEDs) offer for display and lighting applications in terms of brightness, production cost, power consumption, *etc.* are not rivaled by any other technologies today. Consequently, an innumerable number of organic materials have been created in the last two decades for application in OLEDs.[1] Despite this abundance, certain drawbacks such as color drift with time, low lifetimes, gradual diminution of light intensity, *etc.* yet remain with organic materials. There is thus an incessant effort to design and develop new materials that display superior performance when applied in devices. In general, the organic compounds employed for application in OLEDs as hole-transporting materials (HTMs), electron-transporting materials (ETMs) and emissive materials (EMs) should ideally be amorphous, exhibit high glass transition temperatures (T_gs) and thermal decomposition temperatures (T_ds) and display good charge carrier mobilities.[2] It turns out that high T_g is one of the important criteria for organic materials to be employed in multilayer OLED devices. There are a large number of ETMs and EMs for which the T_gs are significantly high.[1] In contrast, the number of HTMs that are synthetically readily prepared are only a few.[3] *N*,*N*′-di(1-naphthyl)-*N*,*N*′-diphenyl-(1,1′-biphenyl)-4,4′-diamine (NPB) and *N*,*N*′-bis(3-methylphenyl)-*N*,*N*′-diphenylbenzidine (TPD) are two most popular commercially-available HTMs. A serious drawback of both of these materials is low T_g. The T_gs for NPB and TPD are 95 [4a] and 60 °C,[4b] respectively, which seemingly owe their origin to the flexible biphenyl core.

We have shown in our recent investigations that Tröger's Base (TB) scaffold can be diligently exploited to create new bifunctional[5a] and host materials[5b] for application in OLEDs. Our premise for development of these materials for OLEDs rested on the following rationale: first, the unique V-shape of TBs is known to promote lattice inclusion of volatile guests,[6] whereby exclusion of the guests from the lattice leads to amorphous behavior. Second, rigidity of the scaffold and high molecular mass *via* its 2-fold functionalization impart high thermal stabilities (T_gs and T_ds).[5] Third, the electron richness of the TB scaffold allows maneuvering of the HOMO levels to aid facile hole transport. Last, the synthetic chemistry of TB functionalization is well known,[7] and permits ready development, in a cost-effective manner, of a family of compounds with subtle structural variations, which permit fine-tuning of properties. We thus surmised that rigidification of the flexible biphenyl core in NPB by TB scaffold should lead to very important HTMs that are structurally analogous to NPB, but endowed with improved thermal properties. Herein, we report the development of two NPB analogs (**TB1–2**) based on the rigid TB scaffold, and contrast their utility as HTMs with NPB by fabricating multilayer OLED devices with two types of emissive materials; while one of the latter is structurally related to TB, the other is widely distinct, *cf.* Fig. 1. It is shown that the readily-synthesized TBs functionalized with *N*-naphthyl-*N*-phenylamines serve as very good HTMs with high T_gs.

The target amines **TB1–2** were prepared starting from 2,8-dibromo-substituted TBs by Buchwald–Hartwig amination protocol, Scheme S1.† The literature-reported procedures[8] involving condensation reaction between 4-bromoaniline or 2-methyl-4-bromoaniline and paraformaldehyde at −78 °C in TFA

[a]*Department of Chemistry, Indian Institute of Technology, Kanpur 208016, India. E-mail: moorthy@iitk.ac.in; Fax: +91 5122597436; Tel: +91 5122597438*

[b]*Department of Electrical Engineering, Indian Institute of Technology, Kanpur 208016, India*

[c]*Institute of Chemistry, Academia Sinica, Taipei, Taiwan 115, Republic of China*

† Electronic supplementary information (ESI) available: Synthesis details and characterization data, ^{1}H and ^{13}C NMR spectral reproductions, TGA and DSC profiles, PXRDs, UV-vis, PL and EL plots/profiles. See DOI: 10.1039/c5ra03391h

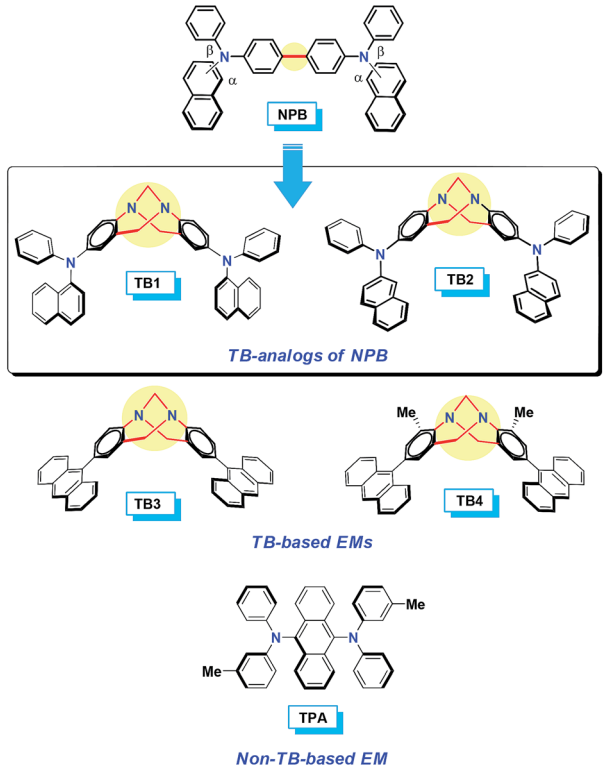

Fig. 1 The structures of α-/β-NPB and TB-functionalized HTMs, namely, **TB1** and **TB2**. Also shown are the structures of TB-based EMs and a non TB-based EM with which the functioning of **TB1–2** and **NPB** as HTMs are contrasted.

afforded the core scaffolds, *i.e.*, 2,8-dibromo-substituted TB and 2,8-dibromo-4,10-dimethyl-substituted TB. Amination of 2,8-dibromo-TB with *N*-phenyl-1-naphthylamine and *N*-phenyl-2-naphthylamine, *cf.* Scheme S1,† yielded TB-amines, *i.e.*, **TB1–2**, in 67–73% yields. The anthracene-functionalized TBs, *i.e.*, **TB3** and **TB4**, were accessed from 2,8-dibromo-substituted TB and 2,8-dibromo-4,10-dimethyl-substituted TB by Pd(0)-catalyzed Suzuki coupling with 9-anthraceneboronic acid in 70–75% yields, Scheme S1.† The non-TB-based amine, *i.e.*, TPA, was procured from a commercial source.

The UV-vis absorption and photoluminescence spectra of **TB1–4** in DCM are shown in Fig. S1.† A careful examination of the normalized absorption and fluorescence spectra of both **TB1** and **TB2** reveals that the linkage isomers exhibit considerable differences in their optical properties. Insofar as their UV-vis absorption spectra are concerned, a structured absorption is clearly apparent for **TB2**, while one observes a broad feature in the case of **TB1**. Similarly, the fluorescence spectra for excitation at 340 nm show slightly different features for the two **TB**s with a red-shifted emission maximum in the case of **TB1** (465 nm) relative to that of **TB2** (446 nm). UV-vis absorption spectra of the anthryl-substituted **TB**s, *i.e.*, **TB3** and **TB4**, is dominated by the absorption pattern of anthracene moiety in the 325–400 nm region. The emission quantum yields for **TB3** and **TB4** were determined in DCM relative to anthracene as the standard, and were found to be 11 and 12%, respectively, *cf.* Table 1.

The HOMO energies of **TB1–4**, obtained from the onset oxidation potentials, were found to be similar (*ca.* 5.0 eV) for all the TBs. The LUMO energies were estimated by subtracting the band gap energies from those of the corresponding HOMOs, *cf.* Table 1. The band gap energies were, in turn, calculated from the red edge absorption onset values. Thermogravimetric and differential scanning calorimetry (TGA and DSC) analyses were performed for TBs at a heating rate of 10 °C min^{-1} under nitrogen gas atmosphere. The data in Table 1 show that all TBs indeed exhibit high thermal decomposition temperatures with T_gs in the range of 152–196 °C, *cf.* ESI.†

As mentioned earlier, high thermal stabilities are very important for application of organic materials in OLEDs. While high decomposition temperature generally ensures thermal stabilities of organic materials employed as thin films, high T_gs allow creation of pin-hole free, stable and glassy layers in the devices. The T_gs observed for **TB1–2** are remarkably higher than those of NPB (95 °C) and TPD (60 °C). Evidently, replacement of the single bond of biphenyl core in NPB with a rigid diazocine framework extant to TB brings about a remarkable improvement of the T_gs for the TB-based NPB-analogs, *i.e.*, **TB1** and **TB2**. The amorphous nature of **TB1–2** is evident from the featureless PXRD patterns, *cf.* Fig. S6.†

Our efforts to contrast the hole-transporting properties of **TB1–2** and NPB by fabrication of double layer devices with Alq_3 as an ETM as well as EM were to no avail; the device performance results were found to be too poor. We believe that the mismatching in the HOMO energy levels of Alq_3 (5.9 eV) and **TB1–2** (5.0 eV), which manifests in a barrier of 0.9 eV, is the cause of the observed poor device performances. The efficiencies of **TB1** and **TB2** as HTMs were thus examined by fabrication

Table 1 Photophysical, electrochemical and thermal properties of TBs

Compound	λ_{max} (UV)[a] (nm)	Band gap[b] (eV)	λ_{max} (PL) sol[a] (nm)	Φ_{fl} soln[c] (%)	HOMO[d]/LUMO[e] (eV)	T_d[f]	T_g[g]
TB1	294	3.07	457	—	5.03/1.96	395	156
TB2	315	3.09	446	—	5.02/1.93	403	152
TB3	262	3.08	427	11	5.03/1.95	408	196
TB4	258	3.07	426	12	5.01/1.94	410	187

[a] Absorption and fluorescence spectra were recorded in dilute DCM solutions (*ca.* 10^{-5} M). [b] Band gap energies were calculated from red edge absorption onset values using the formula $E = hc/\lambda$. [c] Quantum yields were determined for excitation at 341 nm relative to anthracene as the standard. [d] HOMO energies were calculated from onset oxidation potentials in the CV spectra recorded in DCM using 0.1 M n-Bu_4NPF_6 as a supporting electrolyte. [e] LUMO energies were calculated by subtracting the band gap energies from HOMO energies. [f] From TGA. [g] From DSC.

of multilayer devices for electroluminescence by employing TPA (9,10-bis(*N*-phenyl-*N*-(*m*-tolyl))anthracene) as an EM, and TPBi (2,2′,2″-(1,3,5-benzenetriyl)-tris(1-phenyl-1-*H*-benzimidazole)) as an ETM; for TPA, the HOMO lies at 5.5 eV. At the same time, devices were also fabricated wherein TBs were replaced with α-NPB. Thus, the device configuration that was followed to contrast the functional behavior of TBs and NPB was the following: ITO/NPB or **TB1–2** (40 nm)/TPA (20 nm)/TPBi (30 nm)/LiF (1 nm)/Al (150 nm). Green emission with λ_{max} (EL) of 516 nm and CIE co-ordinates of (0.30, 0.60) typical of TPA was captured from all the three devices; indeed the EL spectra of all the devices are nicely superimposable, *cf.* Fig. 2. The results of EL for the three devices are collected in Table 2.

A perusal of the results in Table 2 shows compellingly that external efficiency, power efficiency and luminous efficiency for **TB1–2** as HTMs are comparatively better at low current densities, although the maximum luminance is better for NPB. The energy-level diagram for the devices constructed with TPA as an EM and **TB1–2**/NPB as HTMs is shown in Fig. 3(a). As can be seen, the HOMO level of TPA[9] is closer to that of NPB leading to facile migration of holes from the latter into the former. On the other hand, the HOMO is relatively raised by *ca.* 0.5 eV for hole injection from **TB1–2** into TPA layer. Despite this barrier for hole injection into the emissive layer, the device performance results observed for TBs as HTMs are respectable. We wondered if replacement of TPA with an EM of higher HOMO energy results in a better performance of the devices with **TB1–2** as HTMs. We thus designed two EMs, namely **TB3** and **TB4** (Fig. 1), with high HOMOs based on the TB core itself; of course, we were guided by the fact that functionalization of e-rich TB scaffold with anthracene should lead to materials characterized by high HOMOs. To evaluate efficiencies of **TB1–2** *vis-a-vis* NPB as HTMs, two devices of configurations A and B were fabricated, where (A): ITO/NPB or **TB1–2** (40 nm)/**TB3** (20 nm)/PBD (40 nm)/LiF (1 nm)/Al (150 nm), and (B): ITO/NPB or **TB1–2** (40 nm)/**TB4** (20 nm)/PBD (40 nm)/LiF (1 nm)/Al (150 nm). In these devices, PBD, *i.e.*, 2-(4-biphenylyl)-5-phenyl-1,3,4-oxadiazole, serves as an ETM instead of TPBi. This change was necessitated by the need to ensure better matching of the LUMO levels of **TB3–4** with those of the employed ETMs. The energy level diagram for these devices is shown in Fig. 3(b). The results of EL for all devices are collated in Table 3; the EL spectra and *I–V–L* profiles for both configurations A and B are given ESI.†

It should be mentioned that the EL spectra captured for all the devices of configurations A and B are structured, although one observes only a hint of structuring in the solution state emission and none at all in the solid-state vacuum-sublimed thin films, *cf.* ESI.† Further, the EL emission is found to be red-shifted by *ca.* 35 nm with a slight broadening in the longer wavelength region relative to that in the solution state; in other words, the EL spectra are not comparable to those of the PL spectra of thin films as well as the solution-state emission spectra. What is otherwise noteworthy is the fact that for both NPB and **TB1–2** as HTMs, similar EL spectral features were observed, which eliminates the role of HTMs for the observed structured EL. The latter cannot also be attributed to a combination of emissions arising from two different materials, for PBD is indeed a phosphorescent material and emits too weakly with a maximum at 375 nm.[10] At the moment, the origin of structured EL emission is not immediately apparent to us. Be this as it may, a cursory glance at the results in Table 3 sufficiently brings out the fact that **TB1–2** serve as better HTMs than NPB, even with fabrication of a limited number of devices with **TB3–4** as emitters under similar conditions; of course, structural compatibility between **TB1/2** and **TB3/4** *vis-a-vis* NPB and **TB3/4** contributing to better device results to some degree in the former scenario cannot be ruled out.[11] Further, it should be noted that the device performance results for **TB3–4** as EMs are quite different for a given TB-based HTM, *i.e.*, **TB1** or **TB2**, *cf.* Table 3, although they exhibit similar photophysical properties.

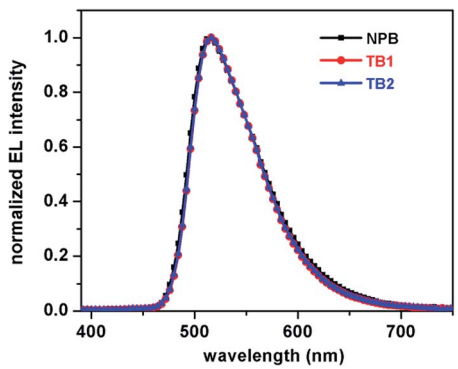

Fig. 2 EL spectra captured from the devices constructed with **TB1–2** and NPB as HTMs and TPA as an EM.

Table 2 Comparison of OLED device performance (electroluminescence) results for NPB and **TB1–2** with TPA as an emissive material[a]

HTMs	V_{on} [b]	η_{ext} [c]	η_p [d]	η_l [e]	λ_{max}^{EL} [f]	L_{max} [g]
NPB	3.0	1.28	3.28	4.34	516	13 240
TB1	3.5	1.6	3.70	5.59	516	8094
TB2	3.5	1.58	4.73	5.39	516	8093

[a] The device configuration was: ITO/NPB or **TB1–2** (40 nm)/TPA (20 nm)/TPBi (30 nm)/LiF (1 nm)/Al (150 nm). [b] Turn-on voltage (V). [c] Maximum external quantum efficiency (%). [d] Maximum power efficiency (lm W^{-1}). [e] Maximum luminance efficiency (cd A^{-1}). [f] λ_{max}^{EL} (nm). [g] Maximum luminance achieved (cd m^{-2}).

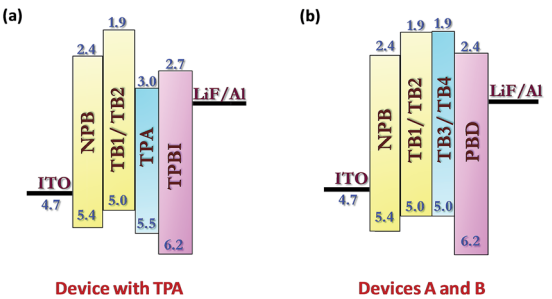

Fig. 3 Relative energy level diagrams for the devices with TPA as an EM (a) and **TB3/4** as an EM (b).

Table 3 Comparison of OLED device performance (electroluminescence) results for NPB and **TB1–2** with **TB3–4** as EMs

HTMs	configuration[a]	V_{on}[b]	η_{ext}[c]	η_p[d]	η_l[e]	λ_{max}^{EL}[f]	L_{max}[g]	CIE[h] (x, y)
NPB	A	3.5	1.80	1.90	2.78	448	886	0.18, 0.21
	B	3.5	1.38	1.05	2.17	448	1070	0.19, 0.21
TB1	A	4.5	2.60	1.95	4.65	452	2254	0.21, 0.25
	B	6.5	0.95	0.59	1.30	448	1205	0.20, 0.25
TB2	A	3.5	1.87	2.11	2.88	448	3422	0.18, 0.20
	B	3.5	1.96	1.59	2.88	448	1430	0.19, 0.19

[a] A and B refer to the device configurations, see text. [b] Turn-on voltage (V). [c] Maximum external quantum efficiency (%). [d] Maximum power efficiency (lm W^{-1}). [e] Maximum luminance efficiency (cd A^{-1}). [f] λ_{max}^{EL} (nm). [g] Maximum luminance achieved (cd m^{-2}). [h] 1931 chromaticity coordinates.

Clearly, subtle structural changes evidently manifest in palpable differences in device results, presumably due to differences in the morphologies of the two materials. Otherwise, it is evident that for configuration A, the device performance results are better for both **TB1** and **TB2** when compared to those for NPB for a wide range of current densities, *cf.* Fig. S12.† One may thus safely conclude that **TB1** and **TB2** should constitute better alternatives to NPB as HTMs with high T_gs, which are ~150 °C; a limitation, however, is that they are applicable to emissive materials with high HOMO energies only. The operational stability of devices is an important aspect that determines longevity of the fabricated devices after repeated use,[12] which has not been investigated by us. It is noteworthy that operational stability of devices is known to benefit, to a large extent, from high T_gs of the employed materials.[13]

Conclusions

We have designed and synthesized novel amorphous hole-transporting materials (HTMs) based on Tröger's Base, *i.e.*, **TB1–2**, as alternatives to the routinely employed NPB. It is shown that the structural rigidity inherent to the TB scaffold manifests in significantly improved T_gs. The hole-transport properties of both **TB1–2** are shown to be comparable to or better than that exhibited by NPB by contrasting the results of device fabrications with two different emissive materials that are TB-based and non-TB-based. The only limitation of both **TB1–2** as HTMs is that they are not applicable to emissive materials with low-lying HOMOs, *e.g.*, Alq_3. Otherwise, their ease of synthesis in conjunction with improved thermal properties should render them much needed alternatives of NPB, which continues to be the best choice of HTMs despite its noted disadvantage of low T_g. We believe that **TB1–2** should constitute invaluable addition to the library of HTMs, which can be readily synthesized.

Acknowledgements

JNM is thankful to SERB (DST), India for generous financial support. IN and SJ gratefully acknowledge Senior Research Fellowships from CSIR, India. We acknowledge the optoelectronic device fabrication and testing by the scientific instrument facility at the Institute of Chemistry, Academia Sinica.

Notes and references

1 (*a*) A. Kraft, A. C. Grimsdale and A. B. Holmes, *Angew. Chem., Int. Ed.*, 1998, **37**, 402; (*b*) M. T. Bernius, M. Inbasekaran, J. O'Brien and W. Wu, *Adv. Mater.*, 2000, **12**, 1737; (*c*) U. Mitschke and P. Bauerle, *J. Mater. Chem.*, 2000, **10**, 1471; (*d*) D. Y. Kim, H. N. Cho and C. Y. Kim, *Prog. Polym. Sci.*, 2000, **25**, 1089; (*e*) Y. Shirota, *J. Mater. Chem.*, 2000, **10**, 1; (*f*) I. D. Rees, K. L. Robinson, A. B. Holmes, C. R. Towns and R. O'Dell, *MRS Bull.*, 2002, **27**, 451; (*g*) L. S. Hung and C. H. Chen, *Mater. Sci. Eng., R*, 2002, **39**, 143; (*h*) A. P. Kulkarni, C. J. Tonzola, A. Babel and S. A. Jenekhe, *Chem. Mater.*, 2004, **16**, 4556; (*i*) G. Hughes and M. R. Bryce, *J. Mater. Chem.*, 2005, **15**, 94; (*j*) T. P. I. Saragi, A. Siebert, T. Fuhrmann-Lieker and J. Salbeck, *Chem. Rev.*, 2007, **107**, 1011; (*k*) Y. Shirota and H. Kageyama, *Chem. Rev.*, 2007, **107**, 953; (*l*) S.-H. Hwang, C. N. Moorefield and G. R. Newkome, *Chem. Soc. Rev.*, 2008, **37**, 2543; (*m*) W.-S. Huang, C.-W. Lin, J. T. Lin, J.-H. Huang, C.-W. Chu, Y.-H. Wu and H.-C. Lin, *Org. Electron.*, 2009, **10**, 594; (*n*) N. Kapoor and K. R. J. Thomas, *New J. Chem.*, 2010, **34**, 2739; (*o*) W. Wei, P. I. Djurovich and M. E. Thompson, *Chem. Mater.*, 2010, **22**, 1724; (*p*) Y. Tao, C. Yang and J. Qin, *Chem. Soc. Rev.*, 2011, **40**, 2943; (*q*) O. Kwon, J. Jo, B. Walker, G. C. Bazan and J. H. Seo, *J. Mater. Chem. A*, 2013, **1**, 7118.

2 Y. Shirota, *Organic Electroluminescence*, ed. Z. H. Kafafi, Taylor & Francis, Washington, DC, 2005, p. 147.

3 For HTMs that are structurally rigid and display high T_g, see: (*a*) H. Zhao, C. Tanjutco and S. Thayumanavan, *Tetrahedron Lett.*, 2001, **42**, 4421; (*b*) C.-W. Ko and Y.-T. Tao, *Synth. Met.*, 2002, **126**, 37; (*c*) Q.-X. Tong, S.-L. Lai, M.-Y. Chan, K.-H. Lai, J.-X. Tang, H.-L. Kwong, C.-S. Lee and S.-T. Lee, *Chem. Mater.*, 2007, **19**, 5851; (*d*) Y.-L. Liao, W.-Y. Hung, T.-H. Hou, C.-Y. Lin and K.-T. Wong, *Chem. Mater.*, 2007, **19**, 6350; (*e*) Z. Chu, D. Wang, C. Zhang, F. Wang, H. Wu, Z. Lv, S. Hou, X. Fan and D. Zou, *Synth. Met.*, 2012, **162**, 614.

4 (*a*) S. A. Van Slyke, C. H. Chen and C. W. Tang, *Appl. Phys. Lett.*, 1996, **69**, 2160; (*b*) K. Naito and A. Miura, *J. Phys. Chem.*, 1993, **97**, 6240.

5 (*a*) I. Neogi, S. Jhulki, A. Ghosh, T. J. Chow and J. N. Moorthy, *Org. Electron.*, 2014, **15**, 3766; (*b*) I. Neogi, S. Jhulki, A. Ghosh, T. J. Chow and J. N. Moorthy, *ACS Appl. Mater. Interfaces*, 2015, **7**, 3298.

6 (*a*) S. Stončius, E. Butkus, A. Žilinskas, K. Larsson, L. Öhrström, U. Berg and K. Wärnmark, *J. Org. Chem.*, 2004, **69**, 5196; (*b*) J. Ashmore, R. Bishop, D. C. Craig and M. L. M. Scudder, *Cryst. Growth Des.*, 2009, **9**, 2742.

7 Ö. V. Rúnarsson, J. Artacho and K. Wärnmark, *Eur. J. Org. Chem.*, 2012, 7015.

8 J. Jensen, M. Strozyk and K. Wärnmark, *J. Heterocycl. Chem.*, 2003, **40**, 373.

9 M.-X. Yu, J.-P. Duan, C.-H. Lin, C.-H. Cheng and Y.-T. Tao, *Chem. Mater.*, 2002, **14**, 3958.
10 K. Goushi, K. Yoshida, K. Sato and C. Adachi, *Nat. Photonics*, 2012, **6**, 253.
11 Structural compatibility between HTM and EM influences the EL performance significantly, see: J. N. Moorthy, P. Venkatakrishnan, P. Natarajan, Z. Lin and T. J. Chow, *J. Org. Chem.*, 2010, **75**, 2599.
12 For operational stability of OLED devices, see: (*a*) K. Okumoto, H. Kanno, Y. Hamma, H. Takahashi and K. Shibata, *Appl. Phys. Lett.*, 2006, **89**, 063504; (*b*) S. H. Cho and M. C. Suh, *Jpn. J. Appl. Phys.*, 2012, **51**, 041601.
13 High T_g has been shown to influence operational stability of fabricated OLED devices, see: (*a*) Y. Kuwubara, H. Ogawa, H. Inada, N. Noma and Y. Shirota, *Adv. Mater.*, 1994, **6**, 677; (*b*) H. Tanaka, S. Tokito, Y. Taga and A. Okada, *Chem. Commun.*, 1996, 2175.